Structural Analysis of *κ*-Carrageenan Sulfated Oligosaccharides by Positive Mode Nano-ESI-FTICR-MS and MS/MS by SORI-CID

Jennifer T. Aguilan and Fabian M. Dayrit
Department of Chemistry, Ateneo de Manila University, Quezon City, Philippines

Jinhua Zhang, Milady R. Niñonuevo, and Carlito B. Lebrilla
Department of Chemistry, University of California at Davis, Davis, California, USA

Structural analysis of sulfated oligosaccharides from *κ*-carrageenan of up to ten residues (MW >2 kDa) was successfully carried out by positive mode nano-ESI-FTICR-MS together with MS/MS using sustained off-resonance irradiation-collision induced dissociation (SORI-CID). Glycosidic bond cleavage reactions via the *B*- and *Y*-types of fragmentation were observed and enabled complete sequencing of the oligosaccharide samples. The positions of the labile sulfate substituents were observable using SORI-CID, enabling the determination of the sequence of the sulfated residues.   (J Am Soc Mass Spectrom 2006, 17, 96–103) © 2005 American Society for Mass Spectrometry

In the last decade, mass spectrometry has emerged as an important tool for the analysis of biomolecules [1]. While most of the attention has been focused on proteins, there is a growing interest in the analysis of carbohydrates. Carbohydrates, however, are difficult to analyze because of their structural heterogeneity, labile substituents, and linkage isomerism.

One of the techniques being explored for the analysis of carbohydrates is nanoelectrospray ionization mass spectrometry (nanoESI-MS) [2, 3]. This technique offers high sensitivity with a detection limit down to 10^{-8} M [4]. In addition, it is a soft ionization technique that is ideal for polysaccharides with labile substituents. Since nano-ESI requires only a small amount of sample, a number of experiments such as high-resolution and collision-induced dissociation (CID or MS/MS) determinations can be performed with 1 *pico*mole [2]. Nano-ESI can be coupled to different mass analyzers such as quadrupole time-of-flight (qTOF,) ion trap, triple quad, and Fourier transform ion cyclotron resonance-mass spectrometry (FTICR-MS) [5–9].

FTICR-MS is advantageous because it can analyze large compounds and is able to achieve high mass resolution with a mass error of less than 1.5 ppm [8, 9]. Sustained off-resonance irradiation (SORI) is a CID method that is often used with FT-ICR [9, 10]; SORI-CID involves irradiation of the ion slightly off its resonance frequency causing the acceleration and deceleration of

ions during the RF pulse at a constant pressure of collision gas. At a frequency of several kilohertz, multiple low-energy collisions occur as ions are vibrationally excited for a sustained period (0.5–1 s).

Sulfated oligosaccharides, such as carrageenans and glycosaminoglycans [11], are difficult to analyze because of the lability of the sulfate substituents. Previous analyses of these sulfated carbohydrates have used FAB, MALDI, and ESI-MS involving either on-line or off-line separation of components in a mixture [11]. It was observed that sodium and ammonium salts of sulfated oligosaccharides, such as heparin, are more stable to desulfation than the free acid forms [12]. It was suggested that Na^+ stabilizes the ion by binding itself in a bidentate or multidentate fashion to the negatively charged $R\text{-}OSO_3^-$ groups [13].

Carrageenans, which are obtained from red seaweed, belong to a class of sulfated polysaccharides and are widely used in biomedical, food, and non-food applications. Recently, *κ*-carrageenan oligosaccharides were reported to behave as elicitors in the cell–cell recognition process that involve host-pathogen interactions in marine plants [14].

The basic carrageenan structure is a disaccharide-repeating unit of a 3-linked *β*-D-galactopyranosyl residue and a 4-linked 3,6-anhydro-*α*-D-galactopyranosyl residue [15–17]. There are about 15 idealized structures identified by Greek letters that differ depending on the presence of the 3,6-anhydro bridge and the position of sulfate substituents [18]. Both the 3,6-anhydro bridge and the sulfate groups are important in determining its tertiary structure and physical properties [17]. Carrageenans have heterogeneous structures that can vary

Table 1. List of sulfated oligosaccharides (as sodium salt from Dextra Laboratories, UK)

Compound	Sulfated oligosaccharide	DP[a]	Nominal MW
1	Neocarrabiose-4[1]-monosulfate: A-G4SNa	1	426.044
2	Neocarratetraose-4[1,3]-disulfate: A-G4SNa-A-G4SNa	2	834.078
3	Neocarratetraose-4[1]-monosulfate[b]: A-G-A-G4SNa	2	732.139
4	Neocarrahexaose-4[1,3,5]-trisulfate: A-G4SNa-A-G4SNa-A-G4SNa	3	1242.112
5	Neocarrahexaose-2[4],4[1,3,5]-tetrasulfate[c]: A-G4SNa-A2SNa-G4SNa-A-G4SNa	3	1344.051
6	Neocarradecaose-4[1,3,5,7,9]-pentasulfate: A-G4SNa-A-G4SNa-A-G4SNa-A-G4SNa-A-G4SNa	5	2058.180

[a]DP: degree of polymerization or the number of disaccharide repeating units.
[b]Has no sulfation on carbon number 4 of the third 3,6-anhydrogalactopyranosyl residue (4[3]).
[c]Has an extra sulfation on carbon number 2 of the fourth 3,6-anhydrogalactopyranosyl residue (2[4]).

according to the algal species, life stage, and processing procedure [14]. Hence, structural analysis is essential for predicting structure-function relationships for these sulfated polysaccharides.

The constituent sugars and linkage positions of carrageenans have been determined by GC-MS analysis of its derivatized alditol acetates and partially methylated alditol acetates. This technique also enables the determination of the position of the sulfate substituent within the sugar residue [19].

The use of soft ionization techniques, such as MALDI and ESI, in the positive and negative modes, together with MS/MS fragmentation, have provided important strategies for determination of sulfate substitution patterns from different types of κ-carrageenan [13, 14, 16, 17, 20–22]. The presence of sulfate substituents in κ-carrageenan makes it amenable to analysis by MALDI and ESI-MS in the negative mode. MS/MS analysis by CID were also performed using ESI-MS the negative

mode for DP = 1–3 [21]. However, because the sulfate substituent is labile, it can be lost by expulsion as HSO_4^-, $NaSO_3$ or $NaHSO_4$, or by in-source fragmentation [13, 21, 22]. Hence, structural information can also be lost.

Recently, Antonopoulos and coworkers reported on the use of ESI-MS with ion-pair reversed-phase liquid chromatography (IP-RPLC) for the analysis of κ-carrageenan oligosaccharides in the positive mode [14]. IP-RPLC achieved the separation of carrageenan oligosaccharides with a degree of polymerization (DP) from 2 to 9, and the molecular ions were observed as single (DP = 2 to 3), double (DP = 4 to 8) and triple (DP = 9) charge states by ESI-MS. However, no MS/MS analysis was performed to obtain further sequence information.

This paper describes the structural analysis of κ-carrageenan oligosaccharide standards (DP = 1 to 5) by positive mode using nano-ESI-FTMS and MS/MS analysis using SORI-CID.
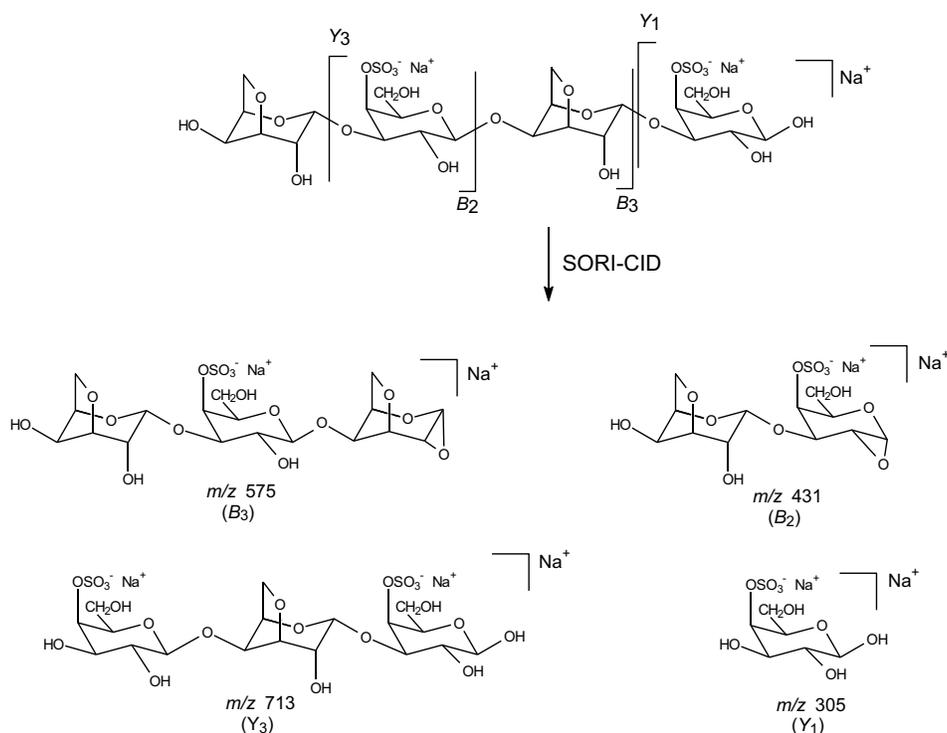

Scheme 1. *B*- and *Y*-fragmentation for neocarratetraose-4[1,3]-disulfate (**2**).

Table 2. Positive mode nano-ESI-FTICR-MS of the neocarraoligosaccharide standards

Sulfated oligosaccharide	Type of ion	Assignment	% Relative intensity	Observed (m/z)	Calculated (m/z)
Neocarrabiose-4^1– monosulfate (**1**)	$[MNa + Na]^+$	$[(A\text{-}G4SNa) + Na]^+$	10	449.034	449.034
	$[2MNa + Na]^+$	$[2(A\text{-}G4SNa) + Na]^+$	100	875.056	875.078
	$[3MNa + Na]^+$	$[3(A\text{-}G4SNa) + Na]^+$	12	1301.093	1301.123
Neocarratetraose-$4^{1,3}$–disulfate (**2**)	$[M2Na + Na]^+$	$[(A\text{-}G4SNa\text{-} A\text{-}G4SNa) + Na]^+$	100	857.048	857.068
	$[M2Na/2 + Na]^+$	$[(A\text{-}G4SNa) + Na]^+$	4	449.034	449.034
Neocarratetraose-4^1–monosulfate (**3**)	$[MNa + Na]^+$	$[(A\text{-}G\text{-}A\text{-}G4SNa) + Na]^+$	100	755.123	755.129
	$[3MNa + 2Na]^{+2}$	$[3(A\text{-}G\text{-}A\text{-}G4SNa) + 2Na]^{+2}$	12	1121.194	1121.199
	$[4MNa + 2Na]^{+2}$	$[4(A\text{-}G\text{-}A\text{-}G4SNa) + 2Na]^{+2}$	18	1487.276	1487.268
		$[M+(A\text{-}G4SNa) + Na]^+$	6	1181.180	1181.173
Neocarrahexaose-$4^{1,3,5}$-trisulfate (**4**)	$[M3Na + Na]^+$	$[(A\text{-}G4SNa)_3 + Na]^+$	100	1265.132	1265.102
	$[4(M3Na) + 3Na]^{+3}$	$[4(A\text{-}G4SNa)_3 + 3Na]^{+3}$	6	1679.213	1679.139
	$[3(M3Na) + 2Na]^{+2}$	$[3(A\text{-}G4SNa)_3 + 2Na]^{+2}$	4	1886.214	1886.157
Neocarrahexaose-$2^4,4^{1,3,5}$-tetrasulfate (**5**)	$[M4Na + Na]^+$	$[(A\text{-}G4SNa\text{-}A2S\text{-}G4SNa\text{-}A\text{-}G4SNa) + Na]^+$	100	1367.017	1367.040
Neocarradecaose-$4^{1,3,5,7,9}$-pentasulfate (**6**)	$[M5Na + Na]^+$	$[(A\text{-}G4SNa)_5 + Na]^+$	4	2081.146	2081.169
	$[M5Na + 2Na]^{+2}$	$[(A\text{-}G4SNa)_5 + 2Na]^{+2}$	100	1052.061	1052.079
	$[2(M5Na) + 3Na]^{+3}$	$[2(A\text{-}G4SNa)_5 + 3Na]^{+3}$	5	1395.093	1395.109

Experimental

Sample Preparation

Stock solutions (ca. 1000 ppm) of the κ-carrageenan oligosaccharide standards obtained in sodium salt form (Dextra Laboratories, UK) (Table 1) were prepared by dissolving each sample in nanopure water. The use of nanopure deionized water minimized matrix effects.

Nano-ESI-FTMS Analysis

All MS experiments were performed on a HiResESI Fourier-transform mass spectrometer (Ionspec, Irvine, CA) with a 9.4 tesla shielded super-conducting magnet. Sample introduction was done using a Micromass Z-spray source interfaced to a nano-ESI external ion source (New Objective, Woburn, MA). The ESI voltage

Figure 1. SORI-CID of the selected parent ion (m/z 875) of the cluster from neocarrabiose-4^1-monosulfate (**1**). Inset: expansion of m/z 448 to 451 showing mass resolution.

ranging from 1.8 to 2.4 kV was applied to the emitter. The sample cone voltage was 30 V. No nebulizer and desolvation gas was used, and the source temperature was ~80 °C. Each spectrum was taken with one scan with an accumulation time in the accumulation hexapole of 1 s.

The mobile phase was delivered using a binary NanoLC pump (Eksigent Technologies, Livermore, CA). Mobile phase was 1:1 water:acetonitrile, with a flow rate of 100 $nano$L/min.

MS/MS analysis was performed using SORI-CID. The desired ion was isolated in the ion-cyclotron resonance (ICR) cell with the use of an arbitrary waveform generation and synthesizer excitation. The ions were excited +1000 Hz of their cyclotron frequency for 1000 ms at 3 to 8 V (base to peak) depending on the desired level of fragmentation and the size of oligosaccharide. Two argon pulses were used during the CID event to maintain a pressure of 10^{-6} torr. External mass calibration was performed giving a calculated average mass error of 11 ppm, with a range of 0 to 44 ppm.

Results and Discussion

The sulfated oligosaccharides studied in this paper were analyzed as the sodium salt. All of the MS1 spectra showed mostly the peaks due to the precursor ions (intensities $\gg 1 \times 10^6$).

Most of the positive SORI-CID ions can be rationalized through a mechanism which starts from the cationization of the glycosidic oxygen atom by Na^+ giving B- and Y-types of fragmentation. B-fragmentation yields an epoxide at the cleavage site with loss of H_2O, while Y-fragmentation leads to proton transfer to the glycosidic oxygen (Scheme **1**). These types of fragmen-
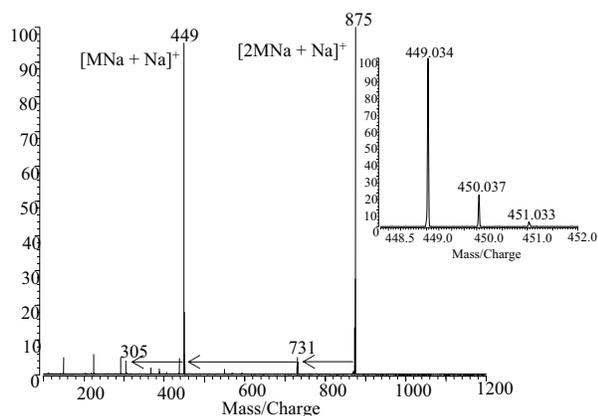
Table 3. MS/MS analysis by SORI-CID of the sulfated oligosaccharide standards

Sulfated oligosaccharide	Parent ion before CID	Assignment of neutral fragment lost	Mass lost (u)	Assignment of fragment ion	Observed (m/z)	Calculated (m/z)	Ion type
Neocarrabiose-4¹–monosulfate (Figure 1)	875.056	[A]	144	[(A-G4SNa) + (G4SNa) + Na]⁺	731.043	731.036	
		[G4SNa]	282	[(A-G4SNa) + Na]⁺	449.036	449.034	
		[A]	144	[(G4SNa) + Na]⁺	304.996	304.992	
Neocarratetraose-4¹,³–disulfate (Figure 2)	857.048	[A]	144	[(G4SNa-A-G4SNa) + Na]⁺	713.018	713.026	Y_3
		[G4SNa]	282	[(A-G4SNa) + Na − H$_2$O]⁺	431.022	431.024	B_2
		[A − H$_2$O]	126	[(G4SNa) + Na]⁺	304.994	304.992	Y_1
	857.048	[G4SNa]	282	[(A-G4SNa-A) + Na − H$_2$O]⁺	575.062	575.066	B_3
		[A]	144	[(A-G4SNa) + Na − H$_2$O]⁺	431.022	431.024	B_2
		[A-H$_2$O]	126	[(G4SNa) + Na]⁺	304.994	304.992	Y_1
Neocarratetraose-4¹–sulfate (Figure 3)	755.123	[A]	144	[(G-A-G4SNa) + Na]⁺	611.094	611.087	Y_3
		[G-A]	306	[(G4SNa) + Na]⁺	304.994	304.992	Y_1
	755.123	[G4SNa]	282	[(A-G-A) + Na − H$_2$O]⁺	473.131	473.127	B_3
		[A]	144	[(A-G) + Na − H$_2$O]⁺	329.091	329.085	B_2
Neocarrahexaose–4¹,³,⁵-trisulfate (Figure 4)	1265.132	[A]	144	[(G4SNa-(A-G4SNa)$_2$) + Na]⁺	1121.055	1121.059	Y_5
		[G4SNa − H$_2$O]	264	[(A-G4SNa)$_2$ + Na]⁺	857.078	857.068	Y_4
		[A]	144	[(G4SNa-A-G4SNa) + Na]⁺	713.027	713.026	Y_3
		[(G2SNa + H$_2$O)]	282	[(A-G4SNa) + Na − H$_2$O]⁺	431.028	431.024	B_2
		[A]	144	[G4SNa + Na]⁺	304.997	304.992	Y_1
	1265.132	[G4SNa]	282	[(A-G4SNa- A-G4SNa-A) + Na − H$_2$O]⁺	983.093	983.099	B_5
		[A]	144	[(A-G4SNa)$_2$ + Na − H$_2$O]⁺	839.055	839.057	B_4
		[G4SNa]	264	[(A-G4SNa)-A) + Na − H$_2$O]⁺	575.065	575.066	B_3
		[A]	144	[(A-G4SNa) + Na − H$_2$O]⁺	431.028	431.024	B_2
		[A − H$_2$O]	126	[(G4SNa) + Na]⁺	304.997	304.992	Y_1
Neocarrahexaose-2⁴,4¹,³,⁵–tetrasulfate (Figure 5)	1367.017	[A]	144	[(G4SNa-A2SNa-G4SNa-A-G4SNa) + Na]⁺	1223.014	1222.998	Y_5
		[G4SNa]	282	[(A2SNa-G4SNa-A-G4SNa) + Na − H$_2$O]⁺	941.007	940.996	B_4
		[A2SNa]	246	[(G4SNa-A-G4SNa) + Na]⁺	695.026	695.020	Y_3
		[(A2SNa-A)]	390	[(G4SNa) + Na]⁺	304.997	304.992	Y_1
	1367.017	[G4SNa]	282	[(A-G4SNa-A2SNa-G4SNa-A) + Na − H$_2$O]⁺	1085.048	1085.038	B_5
		[A]	144	[(A-G4SNa-A2SNa-G4SNa) + Na − H$_2$O]⁺	941.077	940.996	B_4
		[G4SNa − H$_2$O]	264	[(A-G4SNa-A2SNa) + Na]⁺	677.009	677.005	C_3
		[A2SNa]	246	[(A-G4SNa) + Na − H$_2$O]⁺	431.031	431.024	B_2
		[A − H$_2$O]	126	[(G4SNa) + Na]⁺	304.997	304.992	Y_1
Neocarradecaose–4¹,³,⁵,⁷,⁹-pentasulfate (Figure 6)	1052.061			[(A-G4SNa-A) + Na − H$_2$O]⁺	575.065	575.066	B_3
2104 Da [M5Na + 2Na] (deconvoluted)				[(G4SNa-(A-G4SNa)$_3$) + Na]⁺	1529.065	1529.093	Y_7
		[G4SNa]	282	[(A-G4SNa)$_3$ + Na − H$_2$O]⁺	1247.072	1247.091	B_6
		[A − H$_2$O]	126	[(G4SNa-(A-G4SNa)$_2$) + Na]⁺	1121.041	1121.059	Y_5
		[G4SNa]	282	[(A-G4SNa)$_2$ + Na − H$_2$O]⁺	839.051	839.057	B_4
		[A − H$_2$O]	126	[(G4SNa-A-G4SNa) + Na]⁺	713.022	713.026	Y_3
		[G4SNa]	282	[(A-G4SNa) + Na − H$_2$O]⁺	431.025	431.024	B_2
		[A − H$_2$O]	126	[(G4SNa) + Na]⁺	304.993	304.992	Y_1
	1052.061			[(A-G4SNa-A-G4SNa-A-G4SNa-A-G4SNa-A) + Na − H$_2$O]⁺	1799.126	1799.167	B_9
		[A]	144	[(A-G4SNa)$_4$ + Na − H$_2$O]⁺	1655.095	1655.120	B_8
		[G4SNa − H$_2$O]	264	[(A-G4SNa)$_3$-A) + Na − H$_2$O]⁺	1391.109	1391.133	B_7
		[A]	144	[(A-G4SNa)$_3$ + Na − H$_2$O]⁺	1247.072	1247.091	B_6
		[G4SNa − H$_2$O]	264	[(A-G4SNa)$_2$-A) + Na − H$_2$O]⁺	983.087	983.099	B_5
		[A]	144	[(A-G4SNa)$_2$) + Na − H$_2$O]⁺	839.051	839.057	B_4
		[G4SNa − H$_2$O]	264	[(A-G4SNa-A) + Na − H$_2$O]⁺	575.065	575.066	B_3
		[A]	144	[(A-G4SNa) + Na − H$_2$O]⁺	431.025	431.024	B_2
		[A − H$_2$O]	126	[(G4SNa) + Na]⁺	304.993	304.992	Y_1

tation have been proposed to occur in positive CID-MS analysis of oligosaccharides in the presence of Group 1 cations, such as Na^+ [11, 23].

Neocarrabiose (DP = 1)

The mass spectrum of neocarrabiose-4^1-monosulfate (**1**) gave a peak at m/z 449.034 which is assigned to the molecular ion bearing an additional Na^+ ([(A − G4SNa) + $Na]^+$) (Table 2). Higher mass peaks at mz 875.056 and 1301.093 are assigned to ion clusters $[2MNa + Na]^+$ and $[3MNa + Na]^+$, respectively.

MS/MS analysis using SORI-CID on the most abundant ion cluster, m/z 875.056, led to the loss of the 3,6-anhydro-galactopyranosyl residue ([A], 144 u) giving a weak signal at m/z 731.043, which is assigned to the cluster [(A − G4SNa) + (G4SNa) + $Na]^+$. This ion then lost 282 u ([G4SNa]) giving m/z 449.036 ([(A − G4SNa) + $Na]^+$). This further fragmented losing 144 u ([A]) to yield an ion at m/z 304.996, which is assigned as [(G4SNa) + $Na]^+$ (Figure 1 and Table 3).

Neocarratetraose (DP = 2)

Two types of neocarratetraose were analyzed: the "regular" neocarratetraose-4^1, 3-disulfate (**2**), and the "irregular" neocarratetraose-4^1-monosulfate (**3**).

For Compound **2**, the peak with the highest relative abundance was m/z 857.048, corresponding to the molecular ion (Table 2). Fragmentation yielded m/z 449.034 ([(A − G4SNa) + $Na]^+$) from the glycosidic bond cleavage, with loss of 408 u corresponding to half of neocarratetraose, [(A − G4SNa) − H_2O].

The linkage information and the position of the sulfated residue of **2** were deduced from SORI-CID mass spectra using the mechanism of B and Y fragmentations (Figure 2 and Table 3) [24]. We propose that a Y-fragmentation occurred starting from the non-reducing end of the oligosaccharide with loss of 144 u due to the terminal 3,6-anhydrogalactopyranosyl residue ([A]) producing m/z 713.018 ([(G4SNa − A − G4SNa) + $Na]^+$, Y_3 ion). Subsequent loss of 282 u ([G4SNa]) yielded the Y_2 ion (not observed), which fragmented with the loss of water giving the B_2 ion, m/z 431.022 ([(A − G4SNa) + Na − $H_2O]^+$). Finally, loss of 126 u ([A − H_2O]) gave m/z 304.994 ([(G4SNa) + $Na]^+$, Y_1 ion). This clearly shows the sequence and the linkage of the monosaccharide units that make up **2**.

Type B fragmentation of Compound **2** started at the reducing end yielding m/z 575.062 ([(A − G4SNa − A) + Na − $H_2O]^+$, B_3 ion). Subsequent loss of 144 u ([A]) gave m/z 431.022 ([(A − G4SNa) + Na − $H_2O]^+$, B_2 ion). The final fragment, m/z 304.994, is assigned to [(G4SNa) + $Na]^+$ (Y_1).

One of the challenges of structure analysis of κ-carrageenan is to determine whether heterogeneity exists within the fine structure. Accordingly, we used nano-ESI-MS combined with SORI-CID to study a sample of neocarratetraose 4^1−sulfate (**3**). Compound **3** contains a

galactopyranosyl residue that is not sulfated and is therefore a deviation from the ideal structure. The quasimolecular ion, $[MNa + Na]^+$, was found at m/z 755.123, while its clusters give weaker signals (Table 2). The SORI-CID ions of **3** can be rationalized mainly with B and Y fragmentations (Figure 3). Following the B-type of fragmentation, the glycosidic bond of the reducing terminal end cleaved with loss of 282 u ([(G4SNa)]) yielding m/z 473.131 ([(A − G − A) + Na − $H_2O]^+$, B_3 ion) (Table 3). Loss of 144 u ([A]) produced m/z 329.091 ([(A − G) + Na − $H_2O]^+$, B_2 ion). Further loss of 126 u ([A − H_2O]) yielded m/z 203.702, the galactopyranosyl residue [G + $Na]^+$. The signal at m/z 611.094 is assigned to a Y_3 ion, which is formed from the loss of [A] (144 u) at the non-reducing terminal end. Subsequent loss of 306 u ([G − A]) yielded the terminal residue, m/z 304.994 ([(G4SNa) + $Na]^+$, Y_1 ion).

It is noteworthy that Compounds **2** and **3** can be distinguished based on their SORI-CID fragmentations.

Neocarrahexaose (DP = 3)

Two types of neocarrahexaose standards, neocarra-hexaose-$4^{1,3,5}$-trisulfate (**4**) and neocarrahexaose-$2^4,4^{1,3,5}$-tetrasulfate (**5**), were also analyzed. The former sample follows the ideal disaccharide-repeating unit for κ-carrageenan whereas the latter has an extra sulfate substituent at the C-2 position of the 3,6-anhydrogalactropyranosyl residue.

Compound **4** gives a molecular ion at m/z 1265.132 $[M3Na + Na]^+$ (Figure 4). The masses at m/z 1679.213 and m/z 1886.214 were assigned to ion clusters $[4(M3Na) + 3Na]^{+3}$ and $[3(M3Na) + 2Na]^{+2}$, respec-

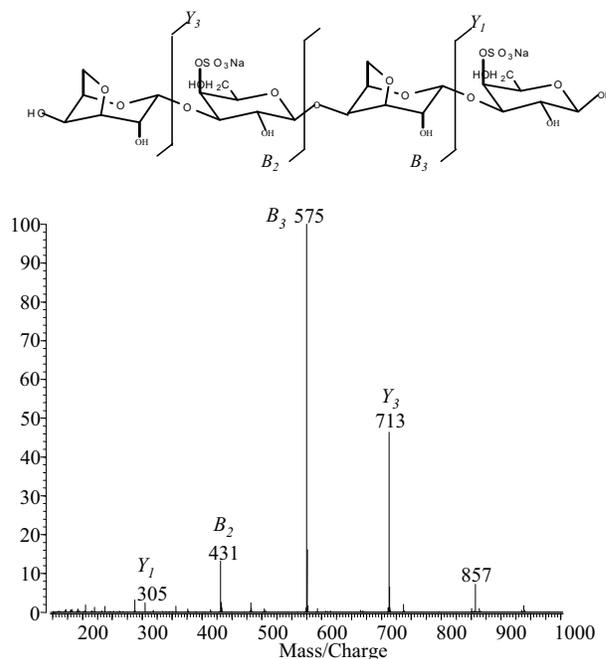**Figure 2.** SORI-CID of the selected parent ion (m/z 857) of neocarratetraose-$4^{1,3}$-disulfate (**2**), $[M(2Na) + Na]^+$.
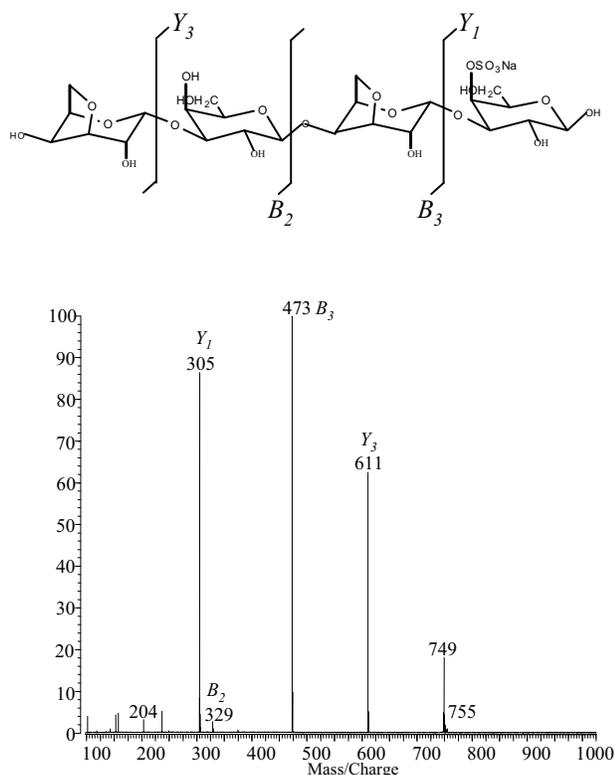
Figure 3. SORI-CID of the selected parent ion (m/z 755) of neocarratetraose-4[1]-monosulfate (**3**), $[M(Na) + Na]^+$.

tively. B fragmentation first proceeded by glycosidic bond cleavage at the reducing end yielding an abundant ion at m/z 983.093 ($[(A − G4SNa − A − G4SNa − A) + Na − H_2O]^+$, B_5 ion). This was followed by sequential fragments at m/z 839.055, ($[(A − G4SNa − A − G4SNa) + Na − H_2O]^+$, B_4 ion), m/z 575.065 ($[(A − G4SNa − A) + Na − H_2O]^+$, B_3 ion), and m/z 431.028 ($[(A − G4SNa) + Na − H_2O]^+$, B_2 ion). Finally, the B_2 ion loses 126 u ($[A − H_2O]$) yielding m/z 304.997 ($[(G4SNa) + Na]^+$, Y_1). This sequential B-type of fragmentation was commonly observed in the "regular" κ-carrageenan oligosaccharides.

Y fragmentation of **4** started from the non-reducing end with Y_5 (m/z 1121.055), Y_4 (m/z 857.078), Y_3 (m/z 713.027), B_2 (m/z 431.028), and Y_1 (m/z 304.997) (Table 3).

Compound **5** gave the parent ion at m/z 1367.017 corresponding to a $[M4Na + Na]^+$ (Table 2). SORI-CID of m/z 1367.017 first produced a fragment at m/z 1085.048, the B_5 ion formed from the loss of $[G4SNa]$ (282 u) at the terminal reducing end (Figure 5 and Table 3). The ion at m/z 941.077, which is assigned to $[(A − G4SNa − A2SNa − G4SNa) + Na − H_2O]^+$ (B_4 ion), confirmed the position of the A2S in the oligosaccharide. Further glycosidic bond cleavages produced m/z 677.009 ($[(A − G4SNa − A2SNa) + Na]^+$, C_3 ion) and m/z 431.031 ($[(A − G4SNa) + Na − H_2O]^+$, B_2 ion). It is worth noting that in the presence of the 2-sulfate substituent, a C-cleavage is favored, which keeps the sulfate group intact. This clearly indicates the exact

position of the (A2SNa) unit in the backbone as the third sugar residue from the non-reducing end.

The Y-type of fragmentation of **5** complimented sequence information obtained from B-type fragmentations. Y fragmentation started with the loss of 144 u ($[A]$) at the non-reducing end yielding m/z 1223.014 (Y_5 ion), followed by the loss of 282 u ($[G4SNa]$) yielding m/z 941.007 (B_4 ion), then the loss of 246 u ($[A2SNa]$) yielding m/z 695.026 (Y_3 ion). Likewise, a B_4 ion was observed due to the presence of A2SNa in the fourth residue from the non-reducing end. The peak at m/z 304.997 was assigned to the final fragment $[(G4SNa) + Na]^+$ (Y_1).

Neocarradecaose (DP = 5)

For the neocarradecaose-4[1,3,5,7,9]-pentasulfate (**6**), a doubly charged ion signal (m/z 1052.061) with highest relative abundance was detected. Deconvolution of m/z 1052.061 gave the true molecular ion at 2104 Da. The MS/MS analysis was performed by SORI-CID of m/z 1052.061. Both B- and Y-type fragmentations were observed (Figure 6, Tables 2 and 3).

We propose that the B-fragmentation started from the unobserved molecular ion, 2104 Da, which first produced m/z 304.993 ($[(G4SNa) + Na]^+$, Y_1 ion) and m/z 1799.126 ($[(A − G4SNa − A − G4SNa − A − G4SNa − A − G4SNa − A) + Na − H_2O]^+$, B_9 ion). On the other hand, Y-fragmentation began with the glycosidic bond cleavage from the non-reducing end producing both m/z 575.065 ($[(A − G4SNa − A) + Na − H_2O]^+$, B_3 ion) and m/z 1529.065 ($[(G4SNa − A − G4SNa − A − G4SNaA − G4SNa) + Na]^+$, Y_7 ion). Both

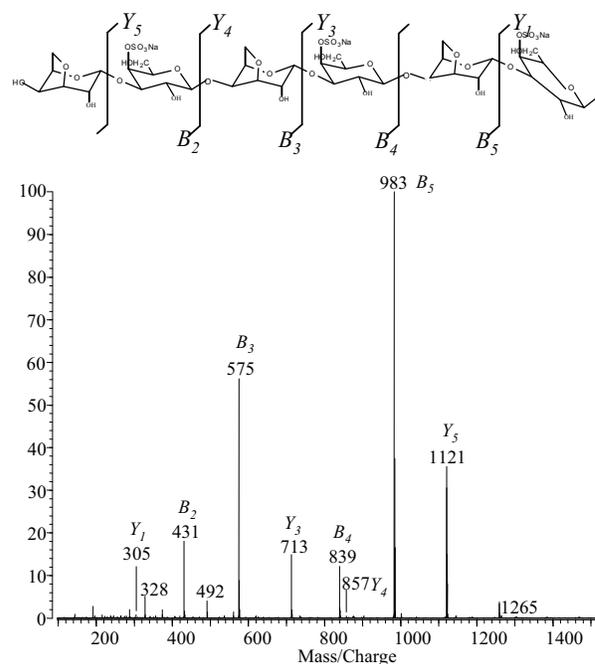**Figure 4.** SORI-CID of the selected parent ion (m/z 1265) of neocarrahexaose-4[1,3,5]-trisulfate (**4**), $[M(3Na) + Na]^+$.
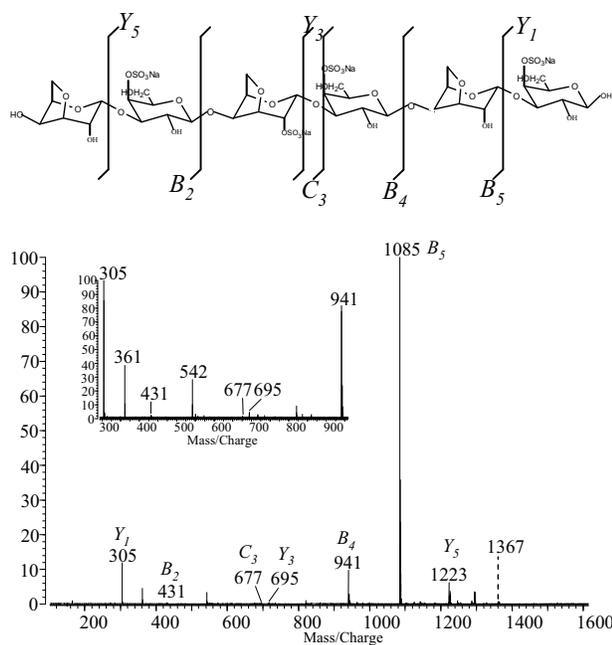
Figure 5. SORI-CID of the selected parent ion (*m/z* 1367) of neocarrahexaose-$2^4,4^{1,3,5}$-tetrasulfate (**5**), $[M(4Na) + Na]^+$.

intermediates eventually underwent fragmentation enabling the complete sequencing of the alternating units of 4-linked 3,6-anhdrogalactopyranosyl and 3-linked galactopyranosyl 4-sulfate residues in neocarradecaose-$4^{1,3,5,7,9}$-pentasulfate. SORI-CID MS/MS gave glycosidic bond cleavage with retention of the sulfate substituents. This allowed the exact assignment of sulfate positions in the κ-carrageenan backbone.

Conclusions

Nano-ESI-FTMS in the positive mode with SORI-CID was successfully used for the structural analysis of κ-carrageenan oligosaccharides ranging from DP = 1 to 5. Glycosidic bond cleavage reactions from the sulfated oligosaccharide backbone occurred mainly via the *B*- and *Y*-types of fragmentation providing complete sequencing of both regular and irregular samples, thus enabling the determination of heterogeneity within a sulfated oligosaccharide backbone. The labile sulfate substituents were retained, enabling the unambiguous determination of the sequence of the sulfated residues.
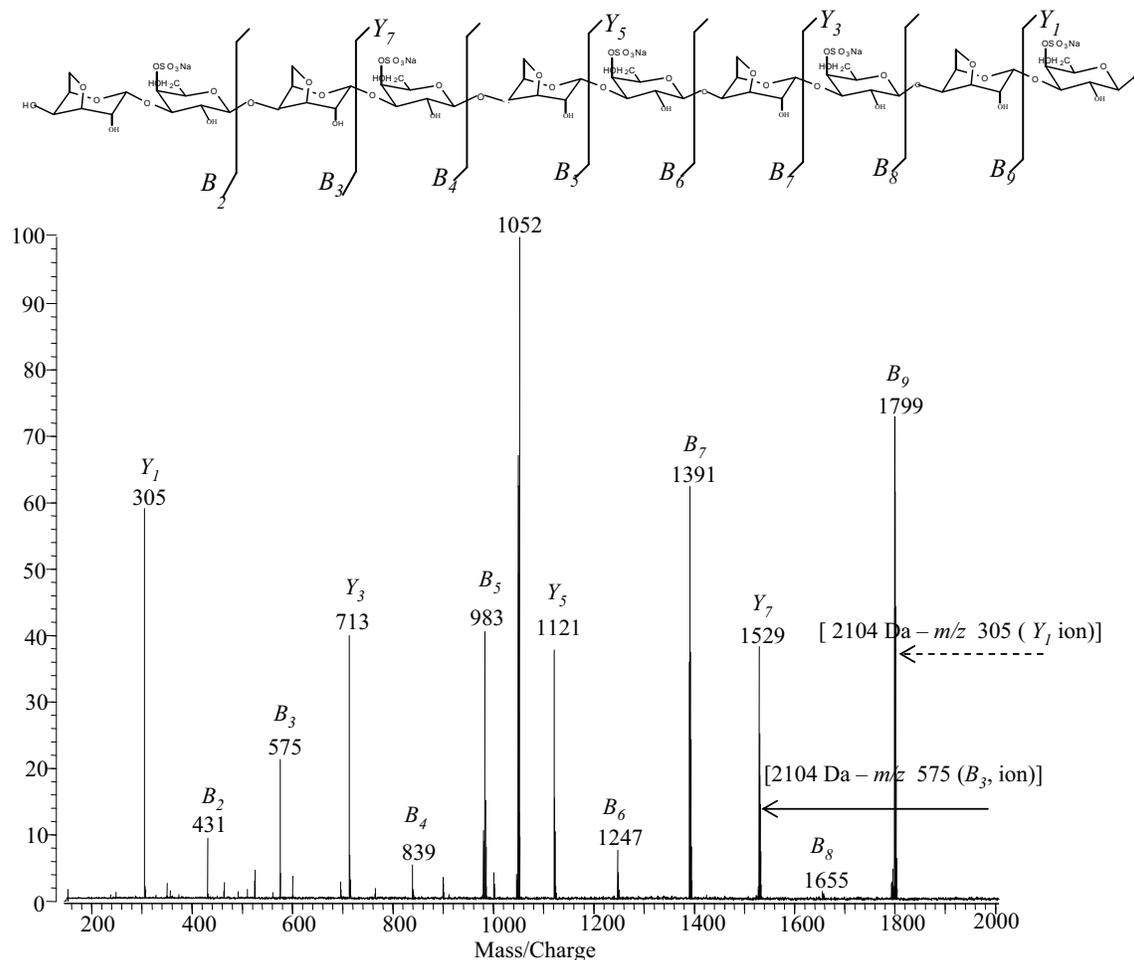

Figure 6. SORI-CID of the selected parent ion (*m/z* 1052) of neocarradecaose-$4^{1,3,5,7,9}$-pentasulfate (**6**), $[M(5Na) + 2Na]^{2+}$. This doubly charged ion was deconvoluted to the true molecular ion ($[M5Na + 2Na]$, 2104 Da).

The high mass accuracy and sensitivity of nano-ESI-FTMS together with the mild collision conditions of SORI-CID proved to be very effective for the analysis of sulfated carbohydrates such as carrageenan. This technique can also be applied to the analysis of other carbohydrates that are difficult to analyze using other MS methods.

Acknowledgments

References

1. McLafferty, F.; Fridriksson, E.; Horn, D.; Lewis, M.; Zubarev, R. Biomolecule Mass Spectrometry. *Science* **1999,** *284* (5418), 1289–1290.
2. Karas, M.; Bahr, U.; Dülcks, T. Nanoelectrospray Ionization Mass Spectrometry: Addressing Analytical Problems Beyond Routine. *Fresenius J. Anal. Chem.* **2000,** *366,* 669–676.
3. Schmidt, A.; Bahr, U.; Karas, M. Influence of Pressure in the First Pumping Stage on Analyte Desolvation and Fragmentation in Nano-ESI MS. *Anal. Chem.* **2001,** *73,* 6040–6046.
4. Wilm, M.; Mann, M. Analytical Properties of the Nanoelectrospray Ion Source. *Anal. Chem.* **1996,** *68,* 1–8.
5. Zamfir, A.; Seidler, D.; Kresse, H.; Peter-Katalinic, J. Structural Investigation of Chondroitin/Dermatan Sulfate Oligosaccharide from Human Skin Fibroblast Decorim. *Glycobiology* **2003,** *13*(11), 733–742.
6. Wang, Y.; Schubert, M.; Ingendok, A.; Franzen, J. Analysis of Noncovalent Protein Complexes up to 290 kDa Using Electrospray Ionization and Ion Trap Mass Spectrometry. *Rapid Commun. Mass Spectrom.* **2000,** *14,* 12.
7. Smith, R.; Loo, J.; Barinaga, C.; Edmonds, C.; Udseth, H. Collisional Activation and Collision Activated Dissociation of Large Multiply Charged Polypeptides and Proteins Produced by Electrospray Ionization. *J. Am. Soc. Mass Spectrom.* **1990,** *1,* 53–65.
8. Hofstadler, S.; Griffey, R.; Pasa-Tolic, L.; Smith, R. The Use of a Stable Internal Mass Standard for Accurate Mass Measurements of Oligonucleotide Fragment Ions Using Electrospray Ionization Fourier Transform Ion Cyclotron Resonance Mass Spectrometry with Infrared Multiphoton Dissociation. *Rapid Commun. Mass Spectrom.* **1998,** *12,* 1400–1404.
9. Park, Y.; Lebrilla, C. Application of Fourier Transform Ion Cyclotron Resonance Mass Spectrometry to Oligosaccharides. *Mass Spectrom. Rev.* **2004,** in press.
10. Gauthier, J.; Trautman, T.; Jacobson, D. Sustained Off-Resonance Irradiation for Collision-Activated Dissociation Involving Fourier Transform Mass Spectrometry. Collision-Activated Dissociation Technique that Emulates Infrared Multiphoton Dissociation. *Anal. Chim. Acta* **1991,** *246,* 211–225.
11. Zaia, J. Mass Spectrometry of Oligosaccharides. *Mass Spectrom. Rev.* **2004,** *23,* 161–227.
12. Chai, W.; Luo, J.; Lim, C. K.; Lawson, A. M. Characterization of Heparin Oligosaccharide Mixtures as Ammonium Salts Using Electrospray Mass Spectrometry. *Anal. Chem.* **1998,** *70,* 2060–2066.
13. Ackloo, S.; Terlouw, J.; Ruttink, P.; Burgers, P. Analysis of Carrageenan by Matrix-Assisted Laser Desorption/Ionization and Electrospray Ionization Mass Spectrometry. I. κ-Carrageenan. *Rapid Commun. Mass Spectrom.* **2001,** *15,* 1152–1159.
14. Antonopoulos, A.; Favetta, P.; Helbert, W.; Lafosse, M. Isolation of κ-Carrageenan Oligosaccharides Using Ion-Pair Liquid Chromatography-Characterization by Electrospray Ionization Mass Spectrometry in Positive Ion Mode. *Carboydr. Res.* **2004,** *339,* 1301–1309.
15. Trono, G. C. Jr. *Field Guide: Atlas of the Seaweed Resources of the Philippines;* National Bookstore, Inc.: Manila, Philippines, 1997; pp 222–232.
16. Aguilan, J. T.; Broom, J. E.; Hemmingson, J. A.; Dayrit, F. M.; Montano, M. N. E.; Dancel, M. C. A.; Ninonuevo, M. R.; Furneux, R. H. Structural Analysis of Carrageenan from Farmed Varieties of Philippine Seaweed. *Bot. Marina* **2003,** *46,* 179–192.
17. Therkelsen, G. H. In *Industrial Gums Polysaccharide Derivatives,* 3rd ed.; Whistler, R. L.; Be Miller, J. N. Eds.; Academic Press: San Diego, 1994; pp 145–180.
18. Knutsen, S.; Myslabodski, B.; Larsen, B.; Usov, A. A Modified System of Nomenclature for Red Alagal Galactans. *Bot. Marina* **1994,** *37,* 163–169.
19. Stevenson, T.; Furneaux, R. Chemical Methods for the Analysis of Sulphated Galactans from Red Algae. *Carbohydr. Res.* **1991,** *210,* 277–298.
20. Fukuyama, Y.; Ciancia, M.; Nonami, H.; Cerezo, A.; Erra-Balsells, R.; Matulewics, M. Matrix-Assisted Ultraviolet Laser Desorption Ionization and Electrospray Ionization Time of Flight Mass Spectrometry of Sulfated Neocarrabiose Oligosaccharides. *Carbohydr. Res.* **2002,** *337,* 1553–1567.
21. Ekeberg, D.; Knutsen, S.; Sletmoen, M. Negative Electrospray Ionization-Mass Spectrometry (ESI-MS) as a Tool for Analyzing Structural Heterogeneity in κ-Carrageenan Oligosaccharides. *Carbohydr. Res.* **2001,** *334,* 49–59.
22. Yu, G.; Guan, H.; Ioanoviciu, A.; Sikkander, S.; Thanawiroon, C.; Tobacman, J.; Toida, T.; Linhardt, R. Structural Studies on κ-Carrageenan Derived Oligosaccharides. *Carbohydr. Res.* **2002,** *337,* 433–440.
23. Cancilla, M.; Wong, A.; Voss, L.; Lebrilla, C. Fragmentation Reactions in the Mass Spectrometry Analysis of Neutral Oligosaccharides. *Anal. Chem.* **1999,** *71,* 3206–3218.
24. Domon, B.; Costello, C. E. A Systematic Nomenclature for Carbohydrate Fragmentation in FAB-MS/MS Spectra of Glycoconjugates. *Glycoconj. J.* **1988,** *5,* 397–409.